Dynamic Modeling of Combined Concentrating Solar Tower and Parabolic Trough for Increased Day-to-Day Performance

Georgios E. Arnaoutakis, Dimitris Al. Katsaprakakis, Dimitris G. Christakis
Department of Mechanical Engineering, Hellenic Mediterranean University, Estavromenos, Heraklion Crete 710 04, Greece

Abstract
Concentrating solar power is an important technological option to gradually increase the share of energy produced by renewable energy sources. Central power towers and parabolic trough collectors, are currently the most mature technologies globally installed. While the former technology requires less land area to produce the same power output, the latter operates at lower temperatures thereby requiring less demanding materials. In this paper, we investigate by dynamic modeling the potential of both technologies in the same plant configuration. We find more stable day-to-day annual power profile for a configuration of a 29 MWe tower and 25 MWe of north-south oriented parabolic trough collectors compared to single technology plants. This results in a higher maximum capacity factor of 18% at 925 W/m^2 direct normal irradiance and discounted payback of 9 years at a cost of electricity of 248 Euro/MWh compared to a standalone plant based on parabolic trough technology. In this way, the advantages of both concentrating technologies can be utilized and aid towards wider utilization of solar energy.

1. Introduction
Concentrating solar power (CSP) is one important technology for utilization of the solar energy resource, whilst at the same time increasing the share of energy produced by renewable energy sources. Mature CSP technologies and incentives via feed-in tariffs support rapid development of new power plants. CSP technologies currently at different levels of maturity, are the linear parabolic trough (PTC), the central tower with two-axis tracking heliostats (SPT), the linear Fresnel reflector and the parabolic dish employing a Stirling engine or a micro turbine. The first two technologies with the highest level of maturity currently hold the highest share of installed plants with lowest levelized cost of electricity (LCOE) of 260-370 $/MWh for PTC without storage and 200-290 $/MWh for SPT with 6-7.5 h storage [1].

1.1. Literature review
Despite the extensive deployment of CSP plants, reported field measurements are very limited. Analytical models based on PTC with direct steam generation in the US and Spain, provided adequate performance evaluations of collector, Rankine cycle turbine and system overnight losses [2,3]. Dynamic modeling of PTC plants based on Rankine cycle turbine calculated almost double the solar fraction of the plant by using molten salt storage [4]. In another report [5] the lowest LCOE of a 50 MWe PTC plant was found at a solar multiple, of 2.6 with 16 h and at 1.2 without any storage.
Fewer studies exist comparing the most mature CSP technologies. Ravelli [6] compared PTC and SPT plants at a rated power of 62.1 MWe. By utilising a genetic optimisation algorithm, the design area resulted to approximately 1.8×10^6 m^2 for a north-south oriented PTC, 1.7×10^6 m^2 for an east-west oriented PTC and 10^6 m^2 for a SPT. Moreover, 35% higher storage capacity was required for the north-south oriented PTC compared to the alternatives, explained by increased resource variation between summer and winter months.
Ravelli's results largely agree with Izquierdo [7] based on geographical data in Spain, reporting a higher collectible power per unit area for PTC in the summer and very similar power per unit area for both PTC and SPT plants. Franchini [8] compared PTC and SPT plants with the same area of approximately 10^5 m^2. On one hand they found a 10% higher thermal power for the PTC during

summer months explained by the limited tracking efficiency of the heliostats near zenith hours. In winter months, however, the SPT produces three times the thermal power of the PTC explained by the low incidence angle and lower ambient temperatures. The gross power of the plants was 23.7 MWe and 25.5 MWe for the PTC and SPT, respectively.

1.2. Approach and novelty of combined CSP technologies

Both CSP technologies require considerable land area, that in many locations may be limited due to environmental, infrastructure or financial limitations. Consequently, the available land area can be limited once siting assessments are complete. The performance of a single concentrating solar power technology per plant has been extensively studied, however, more than one technologies can be installed in a plant offering several advantages.

To the best of the authors' knowledge there are very limited reports on CSP plants with combined technologies. In addition, there are very limited reports on experimental data from full scale concentrating solar power plants. Previous investigations on combined technologies applied an analytical model of the heliostat field, the receiver and the storage subsystems, while the calculation of the supercritical coal-fired power plant was performed in Ebsilon Professional. In this way, detailed mass flow rates of superheated and reheated steam could be calculated as a function of the area of troughs for a period of 24 h. The coal consumption rate as a function of heliostats could also be calculated over the same period. This level of detail in the supercritical steam cycle, enabled the detailed design of all subcomponents of the plant. A combined solar tower and trough aided coal-fired plant was reported in [9] with a maximum solar exergy of 69 MW_{th} that is 7.83%-11.88% higher than single technology power plants of the same power. The thermodynamic performance of a 600 MWe combined solar tower and trough power plant with coal assist as the auxiliary source was also reported [10]. Improved power output by increasing the percentage of reheat steam and further increasing the absorbed solar energy, resulted in reduction of carbon dioxide emissions by reduced operation of the coal-fired source. The authors further reported reduced coal consumption by up to 20.3% by additionally using a control model with forecast predictions, thereby adding the ability to store more energy and optimized discharging of thermal energy [11].

Although the benefits in coal consumption by the use of combined technologies were reported for summer and winter solstice, the annual performance and different orientations of the parabolic troughs were not. Especially in the case of locations with highly overcast days, this may lead to overestimation of the annual energy yield. CSP plants are traditionally designed in the power range of several MW. Consequently, a power plant consisting of combined tower and trough technologies, utilizes a specific tower-to-trough power ratio and can be designed according to the schematic in **Figure 1**. Parabolic troughs with horizontal tracking axis can be installed in a north-south or an east-west orientation. Moreover, the performance of combined technologies and their respective financial assessment cannot be estimated with existing software platforms for concentrating solar power. The objectives of this work are the investigation of the optimum tower-to-trough power ratio depending on the orientation of the collectors in terms of annual performance and cost. In this way, the advantages by combination of the technologies are examined, in the first ever CSP power plants in Greece, located in the island of Crete [12].

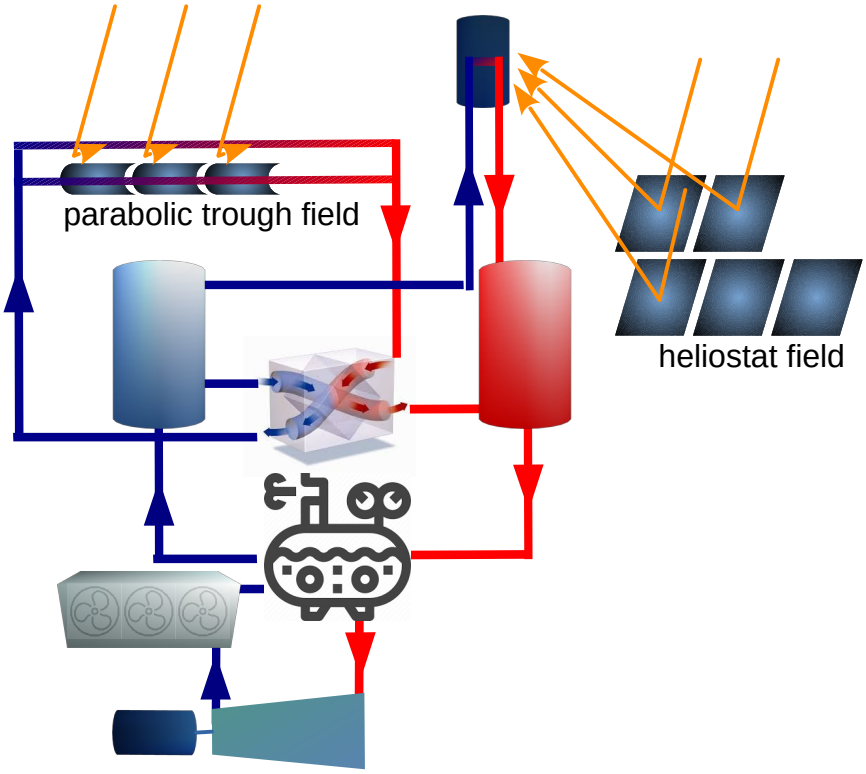

Figure 1: Schematic of the combined concentrated solar thermal power plant configurations consisting of parabolic trough and power tower technologies. Solar energy (orange) is collected by heliostats to the tower and by parabolic troughs and transferred to the heat transfer media operating between low (blue) and high temperatures (red).

2. Methodology

CSP plants primarily collect the sunlight's direct irradiance I_b. For clear skies we modeled the direct irradiance based on the Perez-Ineichen model [13]. The heat input Q_{in} impinging on the solar collectors was calculated as [3]:

$$Q_{in} = I_b \, cos\theta_i \, \eta_{opt} \, A_c \qquad \text{(Equation 1)},$$

Where θ_i is the incidence angle and η_{opt} is the optical efficiency of the receiver. The dimensionless geometrical solar concentration C_{geo} could be calculated as the ratio of the area of collectors A_c and receivers A_r as,

$$C_{geo} = \frac{A_c}{A_r} \qquad \text{(Equation 2)}.$$

The collection efficiency of parabolic troughs varies with incidence angle θ_i. For several parabolic trough technologies the incidence angle modifier $K(\theta_i)$ has been widely reported [5,14,15]. In this treatment, we apply the expression in terms of:

$$K_{\theta_i} = cos\theta_i - 5.25097 \; 10^{-4} \; \theta_i - 2.859621 \; 10^{-5} \; \theta_i^2 \qquad \text{(Equation 3)}.$$

For the solar tower, the following analytical expression was developed based on the field efficiency of central receivers designs [16] as a function of zenith angle in degrees optimized at latitudes of 35°:

$$K_{\theta_\zeta} = 1.6674\ 10^{-1} + 1.4151\ 10^{-2}\theta_\zeta – 9.5178\ 10^{-5}\theta_\zeta^2 \quad \text{(Equation 4).}$$

The data obtained by the fitting function are shown in **Figure 2**. This efficiency incorporates the effect of the cosine of the incidence angle, tower shadowing, atmospheric attenuation and intercept factor between heliostat and receiver.

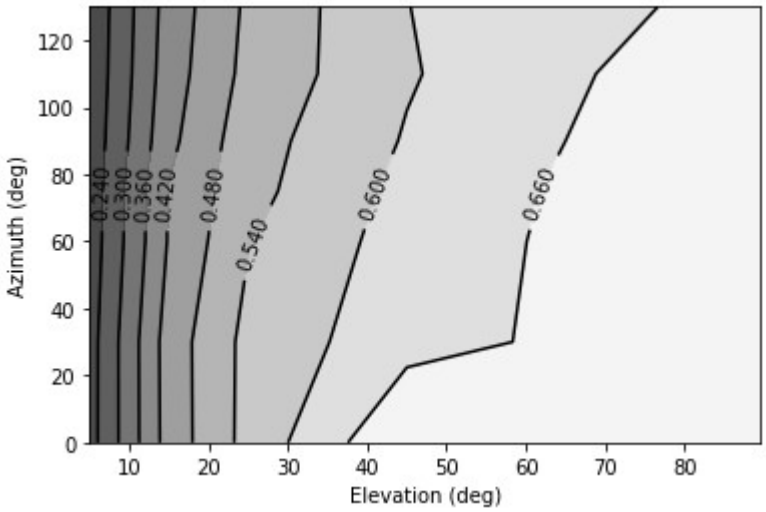

Figure 2: Field efficiency of concentrating solar tower optimized for latitude of 35° [16].

Consequently, the net heat input available to produce work W was calculated as:

$$Q_{net} = \alpha\ Q_{in} - Q_{rad} - Q_{conv} \quad \text{(Equation 5),}$$

Where

$$Q_{rad} = \epsilon\sigma A_r T_r^4 \quad \text{(Equation 6),}$$

Is the radiative flux and Q_{conv} is the convective flux to the environment, while α and ε are the absorptivity and emissivity of the receiver, respectively. For parabolic troughs the convective loss is considered here negligible, however, for solar towers an empirical relation exists, that is [17]:

$$Q_{conv} = \frac{T_r}{60} + \frac{5}{3} \quad \text{(Equation 7).}$$

The work W produced by the turbine of the power block operating was finally calculated from the net heat input and the isentropic efficiency of the Rankine cycle and the efficiency of the generator η_G as:

$$W = Q_{net}\frac{h_i - h_o}{h_i - h_{os}}\eta_G \quad \text{(Equation 8).}$$

The heat losses of the storage system and the pipes connecting the system all together were considered based on the empirical relation:

$$Q_{pi} = 0.01693T - 0.0001683T^2 + 6.78\ 10^{-7}T^3 \quad \text{(Equation 9).}$$

, where

$$\Delta T = \frac{T_{out} + T_{in}}{2} - T_{amb} \quad \text{(Equation 10).}$$

The discounted payback period DPB, the net present value NPV and the internal rate of return IRR, based on a plant lifetime of 30 years, rates *d* and cash flows *Ft* were calculated as:

$$\sum_{t=0}^{DPB} \frac{F_t}{(1+d)^t} \quad \text{(Equation 11)},$$

$$NPV = \sum_{t=0}^{n} \frac{F_t}{(1+d)^t} \quad \text{(Equation 12)},$$

$$\sum_{t=0}^{n} \frac{F_t}{(1+IRR)^t} = 0 \quad \text{(Equation 13)}.$$

All equations were written in python with a flow chart of the implemented code described in **Figure 3**. The developed code to produce the presented results and figures is available at the following repositories [18,19].

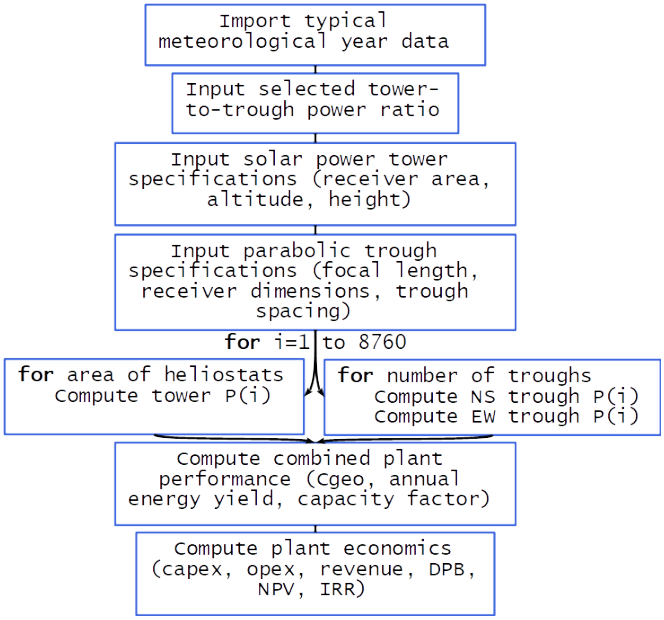

Figure 3: Flow chart of the implemented algorithm for combined concentrating solar power plants

System Advisor Model (SAM) developed by the National Renewable Energy Laboratory (NREL) was utilized for validation of the modeling in the individual technology plants. Simulation of combined plants is not available in SAM. The annual energy of each scenario were validated as displayed in **Figure 4** below. A good agreement was obtained between the trough model and the results of SAM for all the range of power output. A deviation can be seen between the tower model and the results of SAM, especially for plant power below 20 MW and higher than 28 MW. We expect this deviation to be a result of the field efficiency and heliostat area and atmospheric attenuation in our model. A fixed total area of heliostats with unity reflectance and negligible soiling loss was utilized in our model. On the contrary, SAM utilizes an optimization algorithm for each heliostat position based on tower and receiver height for a range of weather conditions on a typical meteorological year. It also consider the facets and canting of each heliostat and considers a sub-unity reflectance, while soiling is removed 60 times a year, within the typical values for optimized cleaning cycles globally [20]. Finally, a polynomial-based atmospheric attenuation was considered in the SAM model averaging to a 6.5% attenuation loss.

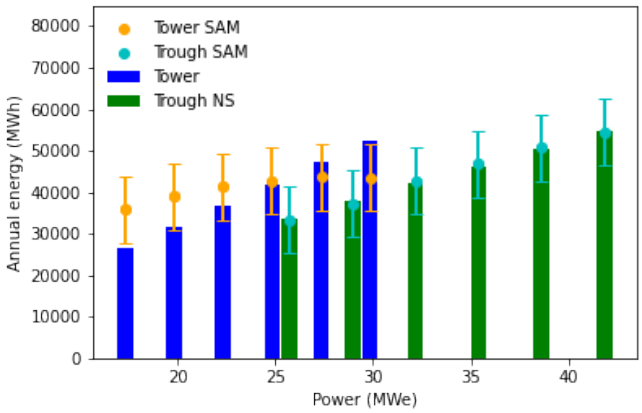

Figure 4: Comparison of the annual energy produced by different scenaria of individual power plants according to the modeling methods utilized herein.

2.1. Case of study

Costs of capital, operation and maintenance of solar concentrating power plants were considered from [21], boilers including efficiencies from [22], while fuel costs from [23]. While costs for site development and heat transfer fluid were 25 euro/m^2 and 60 euro/m^2, respectively, the collector cost embodies the highest development cost at 150 euro/m^2. In addition, the costs of the power block and auxiliary boiler with 40% efficiency were $9.1x10^5$ euro/MWe and $4x10^6$ euro/MWe, respectively. The price of energy was updated based on current regional legislation at 248 euro/MWh with a discount rate of 9%.

Mid-latitude locations experience higher direct irradiance compared to equatorial and subarctic, therefore are preferred. Data of typical meteorological years [24] for locations of 35° latitude were utilized to this end without cloud-induced noise isolation [25], as shown in **Figure 5**. This latitude makes for a case study for the first ever report on concentrated solar power in Greece, located in the island of Crete [12].

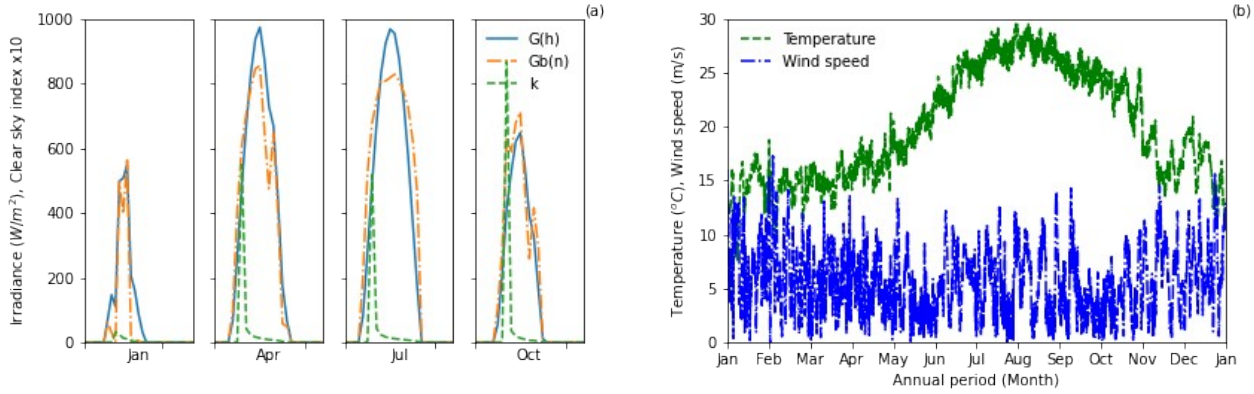

Figure 5: Main weather conditions including a) irradiance, clear sky index and b) temperature and wind speed at the location of the combined concentrating solar power plant.

Plant configurations at several locations along the island were considered. The required demand of the locations based on the population of local communities was further considered. Accordingly, the annual demand varied from averagely populated communities at 8 GWh to 410 GWh for the most densely populated cities in Crete.

Concentrating solar power plant configurations consisting of shared SPT and PTC to produce a minimum power of 50 MWe were investigated. The dimensions of both plants were considered to rely on existing mature SPT and PTC technology. The working fluids were oil and molten salt for parabolic trough and tower plants, respectively. For the tower, a receiver area of 99 m^2 on a 100 m tall tower surrounded by 75 to 125x10^3 m^2 area of heliostats was considered similar to the approach of [26], able to heat the working fluid to a temperature of 565 ^oC. For the parabolic trough collector, a maximum working fluid temperature of 300 ^oC was considered. The parabolic trough collector was 5.76 m wide and 25 m long with focal length of 0.88 m. A linear receiver with outer diameter of 0.07 m, was considered, and a spacing of 18 m between troughs. Scenaria of 800 to 1300 troughs were considered. Molten salt heated by the tower was stored in two tanks, while an oil-to-salt heat exchanger was used to transfer the heat produced by the parabolic troughs into the tanks.

3. Results

3.1. Power profile of standalone plants

Due to the dynamic nature of the solar resource, model development with hourly temporal resolution is required for reliable performance evaluations. The difference in performance between plants is obvious when winter and summer months are compared, displayed for clear sky days in January and August in **Figure 6**. For a typical day in summer the collected irradiance of the PTC plant oriented along north-south, is higher than the energy of the SPT plant. In winter, however, a lower incidence angle reduces the output of the PTC considerably. The collected irradiance of the SPT plant does not change so drastically between seasons. This can be explained as the collection of sunlight by heliostats tracking the sun in zenith and azimuth, that is in three dimensions. The performance of PTC oriented along the east-west is also less affected by the season and the highest collected irradiance is during noon hours. It can be seen that a significant amount of DNI is not collected during morning and afternoon hours, that is higher during summer months. As a result the annual energy yield of the east-west PTC can be less than the north-south orientation.

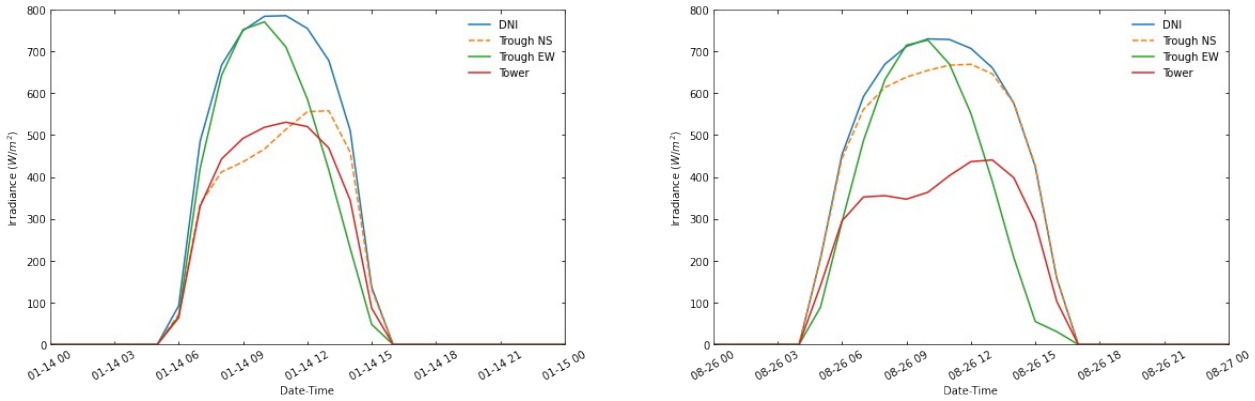

Figure 6: Clear sky energy per unit area of the investigated concentrating solar power plants for January (left) and August (right).

The plants based on a single technology of SPT and PTC required areas of 225,000 m^2 and 259,000 m^2, respectively, for plants of 50 MWe design power output. The annual energy produced by the SPT, the N-S PTC and the E-W PTC was 104,400 MWh, 75,700 MWh and 54,600 MWh, respectively. As shown in **Figure 6**, the limitations of the SPT in summer can be complemented by the PTC and vice versa. Consequently, the seasonal advantages of each technology can be utilized and increase the annual energy yield as well as the day-to-day power production in a combined concentrating solar power configuration. This suggests that a plant comprising of both technologies can entail their mutual advantages and will be investigated in the next section.

3.2. Power profile of combined technologies

How would a combination of both technologies in the plant change the required land area and produced energy? A series of possible configurations within the payback time of a plant were designed by varying the design ratio of power output as displayed in **Figure 7**.

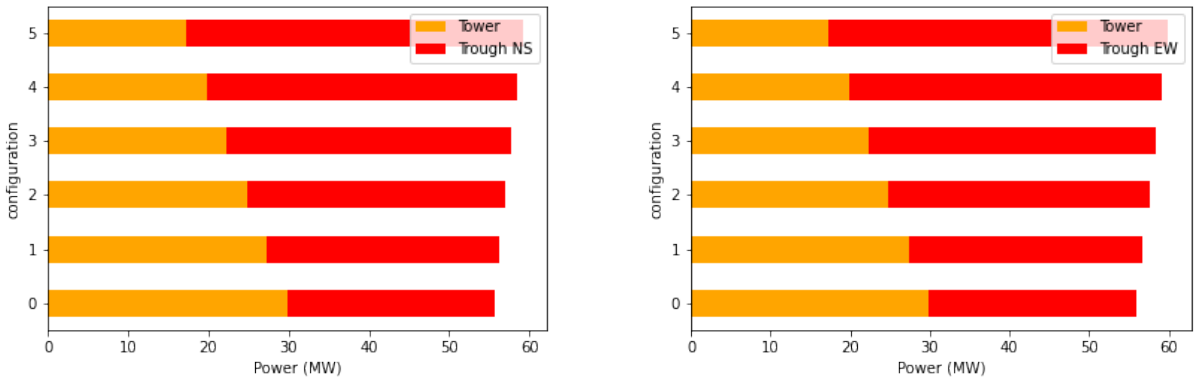

Figure 7: Power of the investigated concentrating solar power plant configurations consisting of solar power tower and north-south (left) or east-west oriented parabolic trough collectors (right). The SPT-to-PTC power ratio was limited to values within the payback time of the plant.

The performance of the configurations is tabulated in Tables 1 and 2, and the optimization curves are displayed in **Figure 8**. Clearly, the configurations with north-south oriented PTC collect and produce a higher amount of annual energy than the configurations with east-west oriented PTC. It can be seen that with lower SPT-to-PTC power ratio, the collector area decreases while the annual energy increases. That is, from 262,200 m^2 to produce 81,129 MWh from 17/41 MWe configuration, to 240,200 m^2 with 86,080 MWh produced by a 29/25 MWe plant. As a result the maximum capacity factor increases from 16% to 18%. The latter configuration consists of SPT and PTC fields with 125,000 m^2 and 115,200 m^2, respectively.

Table 1: Performance characteristics of combined tower and north-south parabolic trough plants

Conf.	Total aperture area (m^2)	Power (MWe)	Annual energy (MWh)	Capacity factor
5	262200	59.18	81129.1	0.16
4	257800	58.47	82119.4	0.16
3	253400	57.75	83109.6	0.16
2	249000	57.04	84099.9	0.17
1	244600	56.32	85090.1	0.17
0	240200	55.60	86080.4	0.18

Table 2: Performance characteristics of combined tower and east-west oriented parabolic trough plants

Conf.	Total aperture area (m^2)	Power (MWe)	Annual energy (MWh)	Capacity factor
5	262200	59.87	65890.8	0.13
4	257800	59.10	68053.2	0.13
3	253400	58.33	70215.6	0.14
2	249000	57.56	72378.1	0.14
1	244600	56.80	74540.5	0.15
0	240200	56.03	76730.0	0.16

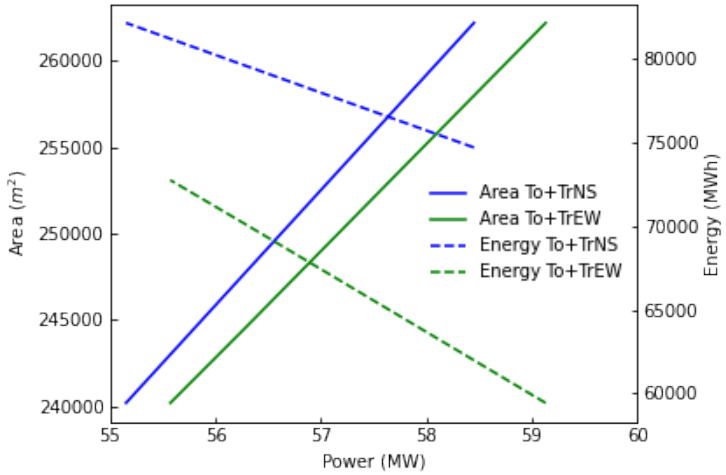

Figure 8: Concentrating solar power plant configurations with respective collector area and annual energy output for a design power higher than 50 MWe. The configuration refer to T+NS for tower and trough NS, while T+EW refers to tower + trough EW.

Figure 9 displays annual maps of the power output of the modeled plants at an hourly temporal resolution. Overcast days, 0-150 and 300-365, do not exhibit significant differences in power output between the plants. It can be seen that all plants exhibit consistently day-to-day higher production during summer days, 150-300, due to a higher frequency of sunny days. During these days, the plants based on tower and parabolic trough in north-south orientation display periodically reduced power output as a result of zenith and incidence angles, respectively. The plant based on east-west oriented

parabolic troughs, is less affected by the incidence angle, while the peak power is centered around noon hours.

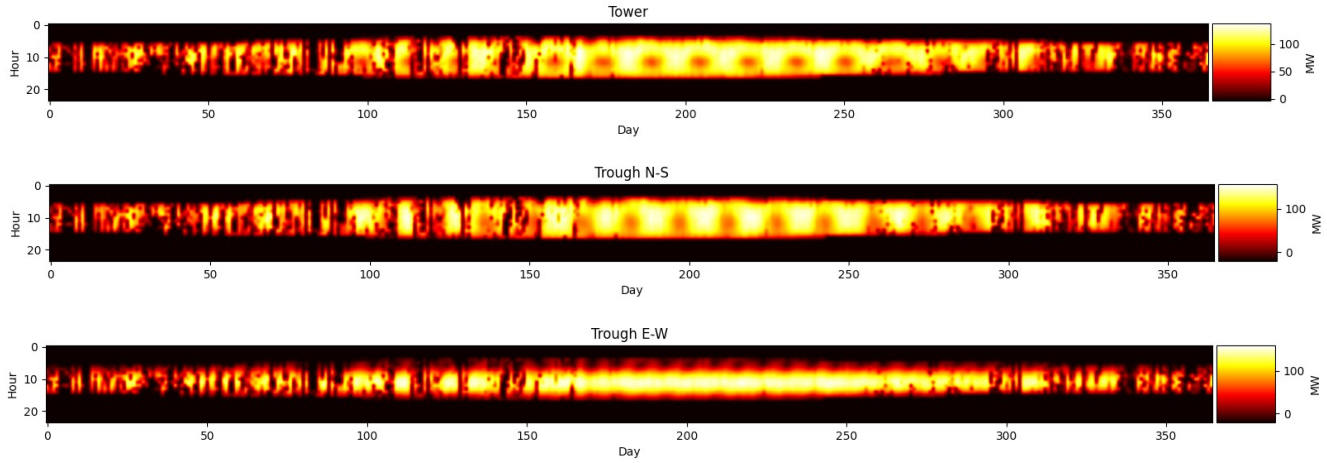

Figure 9: Dynamic hourly thermal power profiles of tower-only (above), north-south (middle) and east-west parabolic trough-only concentrating solar power plants (below).

Crucially, the day-to-day performance of the combined plants produces consistently more power as seen in **Figure 10**. The periodic power fluctuations of the standalone plants, see **Figure 9**, are negated in the combined configurations, resulting in a more stable power profile. In addition, the power produced by the east-west oriented trough is complemented by the tower, resulting in a broader power profile during the day. The produced annual energy is less than a north-south oriented configuration, see Table 2. Nevertheless, a higher power produced during noon hours as shown in **Figure 9**, can be utilized with an east-west configuration.

The features of combined SPT and PTC plant configurations enable a design option, previously unavailable in standalone plants. A more stable day-to-day power profile can be less demanding in storage capacity. Moreover, the amount of auxiliary power required during daily initialization of the plant can be reduced with a more stable profile. The latter is associated with operating costs, that are considered along with the initial costs of the plant in the following section.

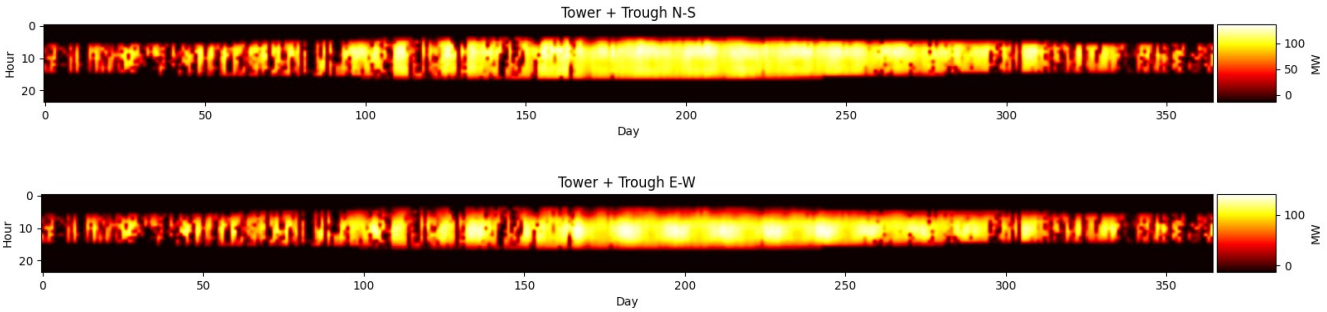

Figure 10: Dynamic hourly thermal power profiles of combined tower with north-south oriented (above) and east-west oriented parabolic trough solar concentrating power plants (below).

3.3. Spatial and financial requirements

The energy produced by the plants should satisfy the initial and recurring cost of the installation. As shown in tables 3, 4 and 5 below, the standalone SPT has lower DPB compared to the standalone PTC plants. For the SPT, with increased aperture area the DPB reduces from 10 to 7 years and is reflected on a higher NPV and IRR when the cost of energy is 248 euro/MWh as a result of increasing produced annual energy from 26,418 MWh to 52,412 MWh.

Table 3: Spatial, performance and financial characteristics of solar power tower scenaria

	0	1	2	3	4	5
Total aperture area (m^2)	75000	85000	95000	105000	115000	125000
C_{geo}	755.28	855.99	956.69	1057.40	1158.11	1258.81
Power (MWe)	17.33	19.84	22.34	24.84	27.35	29.85
Annual energy (MWh)	26418.4	31617.2	36816	42014.7	47213.5	52412.3
Capacity factor	0.1739	0.1819	0.1880	0.1930	0.1970	0.200
DPB (yr)	10.84	9.64	8.88	8.35	7.96	7.67
NPV (euro)	$1.74x10^7$	$2.42x10^7$	$3.11x10^7$	$3.79x10^7$	$4.47x10^7$	$5.15x10^7$
IRR (%)	0.01824	0.03354	0.04748	0.06045	0.07273	0.08449

Table 4: Spatial, performance and financial characteristics of N-S parabolic trough scenaria

	0	1	2	3	4	5
Total aperture area (m^2)	115200	129600	144000	158400	172800	187200
C_{geo}	82.28	82.28	82.28	82.28	82.28	82.28
Power (MWe)	25.75	28.96	32.18	35.40	38.62	41.84
Annual energy (MWh)	33668.1	37876.6	42085.1	46293.6	50502.2	54710.7
Capacity factor	0.1492	0.1492	0.1492	0.1492	0.1492	0.1492
DPB (yr)	15.97	15.78	15.63	15.51	15.41	15.32
NPV (euro)	$1.19x10^7$	$1.38x10^7$	$1.57x10^7$	$1.76x10^7$	$1.95x10^7$	$2.14x10^7$
IRR (%)	0.1159	0.1166	0.1172	0.1177	0.1181	0.1185

Table 5: Spatial, performance and financial characteristics of E-W parabolic trough scenaria

	0	1	2	3	4	5
Total aperture area (m^2)	115200	129600	144000	158400	172800	187200
C_{geo}	82.28	82.28	82.28	82.28	82.28	82.28
Power (MWe)	26.17	29.44	32.71	35.98	39.25	42.53
Annual energy (MWh)	24290.7	27327	30363.3	33399.7	36436	39472.3
Capacity factor	0.1059	0.1059	0.1059	0.1059	0.1059	0.1059
DPB (yr)	15.97	15.78	15.63	15.51	15.41	15.32
NPV (euro)	$1.19x10^7$	$1.38x10^7$	$1.57x10^7$	$1.76x10^7$	$1.95x10^7$	$2.14x10^7$
IRR (%)	0.1159	0.1166	0.1172	0.1177	0.1181	0.1185

The north-south PTC requires 187,200 m^2 to produce 54,710 MWh while the SPT requires 125,000 m^2. This is reflected on the low geometrical concentration of the PTC, that is 82x. The SPT as a point focus technology, can attain geometrical concentration higher than the thermodynamic limit of linear concentrators, and up to several thousand suns depending on the requirements of the heat transfer media [27]. Therefore to produce the same power output and annual energy, less collector area is required. The parametric study presented here focused on a 50 MWe power plant.

It can be seen that the DPB of both PTC plants does not fall below 15 years. The payback can be reduced in combined technology configurations. For the optimum configuration of 29/25 MWe the DPB reduces to 9 years and 12 years for north-south and east-west oriented fields, respectively. In this way, the advantages of the PTC technology can be utilized while maintaining a sustainable plant operation.

Higher cost reductions by fuel saving may be obtained for combined solar power plants of higher capacity [9]. A combined plant approach can aid towards reducing the higher cost of PTC compared to SPT plants that with the addition of storage enable completely renewable electricity [28]. Moreover, a detailed enumeration of all associated costs, can highlight further steps for cost reduction. These costs can refer and are not limited to alternative heat transfer materials [29] and exchanger designs [30,31], steam generator designs [32], pump operation by the application of efficient algorithms, collector cleaning intervals and alternative fuels for auxiliary power. There exist detailed aspects in the power plant that can be improved with the indicated optimization approaches to the thermodynamic and economics. On one hand, the irreversibility of the working fluid either oil or molten salt in the concentration subsystem and the water/steam in the production subsystem can be optimized by minimizing the exergy balance. On the other hand, the total cost of the power plant can be optimized by minimizing the annual capital and operational flows of the expenses. Another important aspect, not analyzed in this manuscript was the environmental impact of the power plant in terms of emitted greenhouse gases. By minimizing the amount of CO_2, CO and NO_x, the environmental impact can be optimized. These aspects favor of novel multi-objective optimization via genetic [33,34] or gray wolf [35] algorithms owing to their successful application in building and cooling systems. Moreover another approach for combined solar thermal plants is coal and lignite gasification. A combined solar thermal plant was calculated to reduce CO_2 emissions by 27% when replacing a combustion-based gasification plant [36]. In a lignite gasification system, the integration of the combined solar thermal input increased the net energy efficiency by 8.3% [37].

4. Conclusions

Configurations of combined concentrating solar power tower and parabolic trough were investigated in this paper. The configurations were designed to produced shared amounts of power to a total of a minimum of 50 MWe. The results of individual plants were validated with System Advisor Model.

An optimum configuration of 29/25 MWe solar power tower-to-parabolic trough was found. This configuration resulted in a maximum capacity factor of 18% compared to 16% of a standalone plant based on a parabolic trough collectors.

This improvement was a result of the concurrent utilization of the collecting efficiency of both technologies. During summer months the collection of the SPT limited by the tracking of solar zenith angle can be complemented by the higher collection efficiency of the PTC. It was shown that during summer months a more stable power profile during the day can be achieved in a combined configuration, regardless of the orientation of the PTC. During winter months, the collection efficiency of the PTC limited by the lower incidence angles can be favorably complemented by the input of the SPT resulting in a more stable day-to-day power output. A more stable daily power profile can be less demanding for the storage as well as the auxiliary power required during the daily initialization of the plant.

The increased collection was also reflected on the spatial and financial specifications of the configurations. By reducing the SPT-to-PTC power ratio from 17/41 MWe to 29/25 MWe, the collector area was reduced and the annual energy was optimized. From an annual energy of 82,129 MWh from 262,200 m^2, the energy increased to 86,080 MWh from an area of 240,200 m^2 consisting of 125,000 m^2 of SPT and 115,200 m^2 of PTC. Due to the reduced area requirements and associated costs, a standalone SPT would require a discounted payback of 7 years. As a result, the discounted payback of a combined plant reduces the payback of a standalone PTC from 15 years to 9 years and 12 years for north-south and east-west oriented PTC, respectively.

Although the presented study focused on the most popular CSP technologies, it can be extended to developing technologies such as the linear Fresnel reflector [38,39] and the parabolic dish [40] offering additional benefits in area optimization and cost. Furthermore, the presented configurations can be supported by combined technology field measurements currently under operation, thereby further aiding the deployment and utilization of solar energy.

Acknowledgments

This research was supported by an academic fellowship of the HMU postdoctoral research program 2020.

CRediT Authorship contribution statement

G.E.A.: Conceptualization, Methodology, Software, Validation, Formal Analysis, Investigation, Resources, Data Curation, Writing – Original Draft, Writing – Review and Editing, Visualization. **D.A.K.**: Writing – Review and Editing, Funding acquisition, Supervision. **D.G.C.**: Writing – Review and Editing, Supervision.

References

1. González-Roubaud, E.; Pérez-Osorio, D.; Prieto, C. Review of Commercial Thermal Energy Storage in Concentrated Solar Power Plants: Steam vs. Molten Salts. *Renewable and Sustainable Energy Reviews* **2017**, *80*, 133–148, doi:10.1016/j.rser.2017.05.084.
2. Fraidenraich, N.; Oliveira, C.; Vieira da Cunha, A.F.; Gordon, J.M.; Vilela, O.C. Analytical Modeling of Direct Steam Generation Solar Power Plants. *Solar Energy* **2013**, *98*, 511–522, doi:10.1016/j.solener.2013.09.037.
3. Salazar, G.A.; Fraidenraich, N.; de Oliveira, C.A.A.; de Castro Vilela, O.; Hongn, M.; Gordon, J.M. Analytic Modeling of Parabolic Trough Solar Thermal Power Plants. *Energy* **2017**, *138*, 1148–1156, doi:10.1016/j.energy.2017.07.110.
4. Mosleh, H.J.; Ahmadi, R. Linear Parabolic Trough Solar Power Plant Assisted with Latent Thermal Energy Storage System: A Dynamic Simulation. *Applied Thermal Engineering* **2019**, *161*, 114204, doi:10.1016/j.applthermaleng.2019.114204.
5. De Luca, F.; Ferraro, V.; Marinelli, V. On the Performance of CSP Oil-Cooled Plants, with and without Heat Storage in Tanks of Molten Salts. *Energy* **2015**, *83*, 230–239, doi:10.1016/j.energy.2015.02.017.
6. Ravelli, S.; Franchini, G.; Perdichizzi, A. Comparison of Different CSP Technologies for Combined Power and Cooling Production. *Renewable Energy* **2018**, *121*, 712–721, doi:10.1016/j.renene.2018.01.074.
7. Izquierdo, S.; Montañés, C.; Dopazo, C.; Fueyo, N. Analysis of CSP Plants for the Definition of Energy Policies: The Influence on Electricity Cost of Solar Multiples, Capacity Factors and Energy Storage. *Energy Policy* **2010**, *38*, 6215–6221, doi:10.1016/j.enpol.2010.06.009.
8. Franchini, G.; Perdichizzi, A.; Ravelli, S.; Barigozzi, G. A Comparative Study between Parabolic Trough and Solar Tower Technologies in Solar Rankine Cycle and Integrated Solar Combined Cycle Plants. *Solar Energy* **2013**, *98*, 302–314, doi:10.1016/j.solener.2013.09.033.

9. Liu, H.; Zhai, R.; Patchigolla, K.; Turner, P.; Yang, Y. Performance Analysis of a Novel Combined Solar Trough and Tower Aided Coal-Fired Power Generation System. *Energy* **2020**, *201*, 117597, doi:10.1016/j.energy.2020.117597.
10. Liu, H.; Zhai, R.; Patchigolla, K.; Turner, P.; Yang, Y. Off-Design Thermodynamic Performances of a Combined Solar Tower and Parabolic Trough Aided Coal-Fired Power Plant. *Applied Thermal Engineering* **2021**, *183*, 116199, doi:10.1016/j.applthermaleng.2020.116199.
11. Liu, H.; Zhai, R.; Patchigolla, K.; Turner, P.; Yang, Y. Model Predictive Control of a Combined Solar Tower and Parabolic Trough Aided Coal-Fired Power Plant. *Applied Thermal Engineering* **2021**, *193*, 116998, doi:10.1016/j.applthermaleng.2021.116998.
12. Katsaprakakis, D.A.; Michopoulos, A.; Skoulou, V.; Dakanali, E.; Maragkaki, A.; Pappa, S.; Antonakakis, I.; Christakis, D.; Condaxakis, C. A Multidisciplinary Approach for an Effective and Rational Energy Transition in Crete Island, Greece. *Energies* **2022**, *15*, 3010, doi:10.3390/en15093010.
13. Perez, R.; Ineichen, P.; Moore, K.; Kmiecik, M.; Chain, C.; George, R.; Vignola, F. A New Operational Model for Satellite-Derived Irradiances: Description and Validation. *Solar Energy* **2002**, *73*, 307–317, doi:10.1016/S0038-092X(02)00122-6.
14. Montes, M.J.; Abánades, A.; Martínez-Val, J.M.; Valdés, M. Solar Multiple Optimization for a Solar-Only Thermal Power Plant, Using Oil as Heat Transfer Fluid in the Parabolic Trough Collectors. *Solar Energy* **2009**, *83*, 2165–2176, doi:10.1016/j.solener.2009.08.010.
15. B, M.G.; F, E.L.; A, R.O.; A, A.E.; C, W.S.; C, A.S.; E, E.Z.; B, P.N. EUROTROUGH- Parabolic Trough Collector Developed for Cost Efficient Solar Power Generation.
16. Rabl, A. *Active Solar Collectors and Their Applications*; Oxford University Press, 1985; ISBN 978-0-19-536521-4.
17. Siebers, D.L.; Kraabel, J.S. *Estimating Convective Energy Losses from Solar Central Receivers*; Sandia National Lab. (SNL-CA), Livermore, CA (United States), 1984;
18. *Combined Concentrating Solar Power Dynamic Model*; https://github.com/olousgap/Combi_CSP;
19. Arnaoutakis, Georgios; Katsaprakakis, Dimitrios *Combined Concentrating Solar Power Dynamic Model*; Mendeley Data, doi: 10.17632/393547xhx2.1, 2022;
20. Ilse, K.; Micheli, L.; Figgis, B.W.; Lange, K.; Daßler, D.; Hanifi, H.; Wolfertstetter, F.; Naumann, V.; Hagendorf, C.; Gottschalg, R.; et al. Techno-Economic Assessment of Soiling Losses and Mitigation Strategies for Solar Power Generation. *Joule* **2019**, *3*, 2303–2321, doi:10.1016/j.joule.2019.08.019.
21. Turchi, C.S.; Boyd, M.; Kesseli, D.; Kurup, P.; Mehos, M.S.; Neises, T.W.; Sharan, P.; Wagner, M.J.; Wendelin, T. *CSP Systems Analysis - Final Project Report*; National Renewable Energy Lab. (NREL), Golden, CO (United States), 2019;
22. *Biomass for Heat and Power*; International Renewable Energy Agency;
23. Crude Oil Prices Weekly 2021 Available online: https://www.statista.com/statistics/326017/weekly-crude-oil-prices/ (accessed on 19 March 2021).
24. Huld, T.; Müller, R.; Gambardella, A. A New Solar Radiation Database for Estimating PV Performance in Europe and Africa. *Solar Energy* **2012**, *86*, 1803–1815, doi:10.1016/j.solener.2012.03.006.
25. Flanagan, R.; Talbot, P.; Osborne, A.; Rabiti, C.; Deinert, M. Isolating Cloud Induced Noise to Improve Generation of Synthetic Surface Solar Irradiances. *Advances in Applied Energy* **2021**, *3*, 100045, doi:10.1016/j.adapen.2021.100045.
26. Avila-Marin, A.L.; Fernandez-Reche, J.; Tellez, F.M. Evaluation of the Potential of Central Receiver Solar Power Plants: Configuration, Optimization and Trends. *Applied Energy* **2013**, *112*, 274–288, doi:10.1016/j.apenergy.2013.05.049.
27. Ho, C.K. Advances in Central Receivers for Concentrating Solar Applications. *Solar Energy* **2017**, *152*, 38–56, doi:10.1016/j.solener.2017.03.048.

28. Kennedy, K.M.; Ruggles, T.H.; Rinaldi, K.; Dowling, J.A.; Duan, L.; Caldeira, K.; Lewis, N.S. The Role of Concentrated Solar Power with Thermal Energy Storage in Least-Cost Highly Reliable Electricity Systems Fully Powered by Variable Renewable Energy. *Advances in Applied Energy* **2022**, *6*, 100091, doi:10.1016/j.adapen.2022.100091.
29. Arnaoutakis, G.E.; Katsaprakakis, D.A. Concentrating Solar Power Advances in Geometric Optics, Materials and System Integration. *Energies* **2021**, *14*, 6229, doi:10.3390/en14196229.
30. Amber, I.; O'Donovan, T.S. Heat Transfer in a Molten Salt Filled Enclosure Absorbing Concentrated Solar Radiation. *International Journal of Heat and Mass Transfer* **2017**, *113*, 444–455, doi:10.1016/j.ijheatmasstransfer.2017.04.028.
31. Flueckiger, S.M.; Iverson, B.D.; Garimella, S.V.; Pacheco, J.E. System-Level Simulation of a Solar Power Tower Plant with Thermocline Thermal Energy Storage. *Applied Energy* **2014**, *113*, 86–96, doi:10.1016/j.apenergy.2013.07.004.
32. González-Gómez, P.A.; Gómez-Hernández, J.; Ruiz, C.; Santana, D. Can Solar Tower Plants Withstand the Operational Flexibility of Combined Cycle Plants? *Applied Energy* **2022**, *314*, 118951, doi:10.1016/j.apenergy.2022.118951.
33. Keshtkar, M.M.; Talebizadeh, P. Multi-Objective Optimization of Cooling Water Package Based on 3E Analysis: A Case Study. *Energy* **2017**, *134*, 840–849, doi:10.1016/j.energy.2017.06.085.
34. Ramos, C.; Barreto, R.; Mota, B.; Gomes, L.; Faria, P.; Vale, Z. Scheduling of a Textile Production Line Integrating PV Generation Using a Genetic Algorithm. *Energy Reports* **2020**, *6*, 148–154, doi:10.1016/j.egyr.2020.11.093.
35. Ghalambaz, M.; Jalilzadeh Yengejeh, R.; Davami, A.H. Building Energy Optimization Using Grey Wolf Optimizer (GWO). *Case Studies in Thermal Engineering* **2021**, *27*, 101250, doi:10.1016/j.csite.2021.101250.
36. Ng, Y.C.; Lipiński, W. Thermodynamic Analyses of Solar Thermal Gasification of Coal for Hybrid Solar-Fossil Power and Fuel Production. *Energy* **2012**, *44*, 720–731, doi:10.1016/j.energy.2012.05.019.
37. Liu, R.; Liu, M.; Zhao, Y.; Ma, Y.; Yan, J. Thermodynamic Study of a Novel Lignite Poly-Generation System Driven by Solar Energy. *Energy* **2021**, *214*, 119075, doi:10.1016/j.energy.2020.119075.
38. Marugán-Cruz, C.; Serrano, D.; Gómez-Hernández, J.; Sánchez-Delgado, S. Solar Multiple Optimization of a DSG Linear Fresnel Power Plant. *Energy Conversion and Management* **2019**, *184*, 571–580, doi:10.1016/j.enconman.2019.01.054.
39. Hertel, J.D.; Canals, V.; Pujol-Nadal, R. On-Site Optical Characterization of Large-Scale Solar Collectors through Ray-Tracing Optimization. *Applied Energy* **2020**, *262*, 114546, doi:10.1016/j.apenergy.2020.114546.
40. Daabo, A.M.; Mahmoud, S.; Al-Dadah, R.K. The Effect of Receiver Geometry on the Optical Performance of a Small-Scale Solar Cavity Receiver for Parabolic Dish Applications. *Energy* **2016**, *114*, 513–525, doi:10.1016/j.energy.2016.08.025.